

CHAPTER 3

ENVIRONMENTAL BASELINE STATUS: PHYSICAL ASPECTS

3.1 GENERAL

Before start of any Environmental Impact Assessment study, it is necessary to determine the baseline levels of relevant environmental parameters, which are likely to be affected as a result of the construction and operation of the proposed Dibang Multipurpose Project. The planning of baseline survey commences from the short listing of impacts and identification of parameters for which the data needs to be collected.

Most of the submergence area falls in the gorge area therefore, it is restricted longitudinally and no major submergence is observed laterally. The length of the reservoir will be 43 km. In such conditions, impacts do not spill over to a large area. Thus, beyond the designated study area, the impacts likely to accrue as a result of project construction and operation are not expected to be significant.

As a part of the study, detailed field studies on various aspects were conducted. Baseline status has been divided into the following three categories:

- Physical aspects
- Ecological aspects
- Socio-economic and ethnographic aspects.

The information presented in this chapter has been collected by the Consultant through field studies, interaction with various government departments and collation of available literature with various institutions and organizations.

3.2 DIBANG CATCHMENT

Dibang Multipurpose Project is located on river Dibang. The river originates from the snow covered southern flank of the Himalayas / Trans Himalayas

close to the Tibet border at an elevation of more than 5000 m. The river Dibang cuts through deep gorges and difficult terrains in its upper reach through the mountains of the Dibang Valley and Lower Dibang Valley districts of Arunachal Pradesh. The total length of Dibang from its source to its confluence with Lohit river at Sadia in Assam is 195 km. The major tributaries of Dibang river are Mathun, Tangon, Dri, Ithun & Emra. A number of small tributaries i.e. Ahi, Ari, Ilu, Ashu, Ephi, Deo etc also join the river. The important feature is that all the tributaries barring Ephi & Deo join Dibang in its hilly catchment. The three major tributaries viz Tangon, Dri and Mathun are almost equal in size because of which the shape of the Dibang catchment is comparatively wide in its upper reach. Out of the total catchment of 11276 sq km (1127600 ha), the directly draining catchment constitutes an area of 59811.88 ha.

3.2.1 Landuse/Land Cover Details

Land use / land cover details of directly draining catchment is shown in Table 3.1 and map 3.1.

Table 3.1: Landuse Details of Directly Draining Catchment

Sl. No.	Class	Area (ha)	Percentage
1	Dense Forest	29163.44	48.76
2	Open Forest	7419.88	12.41
3	Degraded forest / Abandoned Jhum	10281.64	17.19
4	Agriculture / Current Jhum / Habitation	3851.64	6.44
5	Barren / Rocky	7852.32	13.13
6	Water Body	1103.44	1.84
7	Snow	139.52	0.23
	Total	59811.88	100.00

Forest

Dibang catchment is covered by trees and other vegetation types, which are capable of producing timber and other forest produce. The vegetation is

mostly of Northern Tropical Semi Evergreen and North Indian Moist Deciduous Forests. Varying degree of biotic disturbances, mainly due to traditional practice of jhuming has been experienced by few patches of forests. About 48.76 % (29163.44 ha) is dense forest whereas 12.41 % (7419.88 ha) is open forest of total directly draining catchment. In the proposed submergence area the dense mixed forest is limited along the bank of the river.

Settlement and Agriculture

The catchment is lived by rural based settlement only, except few urban areas. Mostly in these areas shifting cultivation is practiced, barring a few patches like Hunli, reach between Ambolin to Anini etc., where terracing is done.

Areas under agriculture / current jhum / habitation works out to be 6.44 % (3851.64 ha) while degraded forest / abandoned jhum works out to be 17.19 % (10281.64 ha) of total area of directly draining catchment.

Snow Covered Area

Snow covered areas constitute about 0.23 % (139.52 ha) of directly draining catchment.

Barren / Rocky Area

Rock exposures of varying lithology, often barren and devoid of soil cover and vegetation or covered with sparse vegetation, are noticed in the directly draining catchment. They occur generally as isolated exposure. The area under this category works out to be 13.13 % (7852.32 ha).

Water Body

Water bodies, mainly comprising of river Dibang and its tributaries, constitute about 1.84 % (1103.44 ha) of total directly draining catchment.

Land use of submergence area

Landuse details of submergence area are presented under Table 3.2 and Map 3.2.

Table 3.2: Landuse of Submergence Area

Landuse class	Area (ha)	Percentage
Abandoned Jhum / Degraded forest	755.26	18.84
Current Jhum / Habitation / Settled cultivation	286.98	7.16
Dense Mixed Forest	1551.76	38.71
Open Forest	619.52	15.45
Rocky	560.42	13.98
Water Bodies	235.06	5.86
Total	4009.00	100.00

3.2.2 Slope

The slope plays a great role for the loss of soil and water from an area and thereby influences its land use capability. Together with the nature and texture of soil, it also determines the erodibility of the soils. In the directly draining catchment five slope categories were identified - Gentle (0 to 15 degrees), Moderate (16 to 30 degrees), Moderately steep (31 to 45 degrees), Steep (46 to 60 degrees), and Very steep (> 60 degrees). The slope details of directly draining catchment are shown in Table 3.3. The slope map of directly draining catchment is placed as Map 3.3.

Table 3.3 : Slope Details of Directly Draining Catchment

Sl No	Degrees	Slope type	Area	Percentage
1	0 to 15	Gentle	12285.88	20.54
2	16 to 30	Moderate	22626.56	37.83
3	31 to 45	Moderately steep	19289.88	32.25
4	46 to 60	Steep	4134.64	6.91
5	> 60	Very steep	1474.92	2.47
			59811.88	100.00

3.2.3 Soils

Soil details of directly draining area are shown in Table 3.12 whereas soil map of directly draining catchment is placed as Map 3.4.

3.2.4 Capability Classification

Studies revealed that for sustained profits all high return land areas should be used only according to its potentiality on long run basis. The Dibang multipurpose reservoir is meant for providing power as well as flood mitigation benefits. The annual normal rainfall in the catchment ranges from 2444 mm to 5399 mm and about 66% of this comes during monsoon (May to September). The intensity of rainfall is as high as 2.0 cm/hour. The silt discharge starts with the monsoon and ends with it. From the land use pattern in the catchment it could be seen that land under forests accounts 96.98%.

In capability classification, lands are divided into two groups, i.e. (a) suitable for cultivation, and (b) unfit for cultivation but suitable for permanent vegetation, namely pastures, orchards and forest vegetation. However, in both the groups, degree of hazards is involved.

In order to provide sustained profits and long-term high return, the capability class of each watershed is worked out. The watershed-wise land capability class is represented in Map 3.5. It is observed that the areas under current and abandoned jhum is grossly mismanaged, misused or even made hazardous mainly due to shift cultivation and that's why it should be brought under permanent terrace cultivation or under silvi-pasture vegetation by persuasion as well as by applying improved technology.

3.2.5 Physiographical, Topographical and Relief Features of the Catchment

Arunachal Pradesh could be divided into four distinct physiographic segments:

- a) Arunachal Himalayan Ranges, that occurs as a "gigantic crescent",
- b) Mishimi Hills, the northern continuation of the Proterozoic succession of Northern Myanmar,
- c) Naga-Patkai Ranges, the eastern extension of Shillong Plateau, and
- d) Brahmaputra Plains.

Further, the Arunachal Himalayan ranges extended from the eastern border of

Bhutan to the Dibang and Lohit Valleys, abutting against

Mishimi Hills, This part is sub-divided into four parallel linear zones:

- a) Tethys or Tibetan Hirnalaya to the north,
- b) Higher Hirnalaya,
- c) Lesser Himalaya, and
- d) Sub-Himalaya to the south.

The hills and mountains in the Tethys Himalaya and Higher Himalaya are made up of Palaeo Proterozoic and Meso Proterozoic rocks, where as those of Lesser Himalaya and Sub-Himalaya are made up of Palaeozoic, Mesozoic, Caenozoic rocks and Noozone - Early Quarternary sediments.

The Dibang Basin lies between Lat 28°11'50" N to 29°25'59" N and Long 95°14'47" E to 96°36'49" E and has a very severe and rigorous topographic feature. Its elevation ranges from 300 m in the outer Siwalik type hills rising from plains of Assam to as high as 5500 to 6000 m in the Greater Himalayas, bordering China.

The upper catchment area is characterized by rugged physiography and can be delineated into Denude Structural Mountains (DSM) and Denudational Mountains (DM). The Piedment Zone is mostly located below EI 400 m, is a stretches of alluvial plains occurring along the foot hills formed by coalescence of several alluvial fans consisting of boulders, stones, pebbles, sand and silt. The Flood Plains are strips of relatively smooth, adjacent to river channels, seasonally flooded, consisting of unconsolidated sediments. The width of the Piedmont Zone, together with Flood Plains, is mostly limit to 12 to 15 km.

The Basin has a catchment area of 11,242 sq km. In the hills, the upper reach of the river is known as R. Mathun, R. Dri and then R. Tangon. As per Agro-climatic Zone, the area falls within (i) Alpine Zone, and (ii) Mild Tropical Plain Zone.

Thus, it can be seen that within the Dibang basin, the hills and mountains occupy nearly 66.7% of the total land area and the relief difference vary from 540 m to 5400 m. The relief map of the entire catchment is incorporated in Map 3.6.

3.2.6 Dibang Catchment Drainage System and Drainage Pattern

The Dibang River is snow as well as rainfed. At its upper reach, it is known as R. Mathun, R. Dri and R. Tangon in chronological descending order. It is known as R. Dibang from the confluence point with R. Ahi. It originates at an altitude of 5355 m to 5375 m in the glacial ranges of Great Himalayas and flows in a general southward direction. The basin is fan shaped, where the tributaries are distributed in such a way that the distances from source to point of confluence are more or less same. Due to such characteristics, the time of concentration of runoff from the tributaries is almost simultaneous, which creates a sudden rise in flow.

The drainage pattern is, pre-dominantly dendritic (tree - like) to trellis (lattice) type as it branches at random, apparently with no definite preference for anyone direction and minor branches flow into another at every conceivable angle. Further, the pattern of tributaries can be distinguished by the pre-dominance of one particular orientation, which is followed by some of the watercourses towards one side and by others to the opposite side with a right angle orientation. The drainage pattern of Dibang catchment is shown in Map 3.7.

The rock formations are homogeneous to folded dipping and the permeability is low to medium, which is indicated by fine drainage texture of dendritic-trellis pattern. The drainage areas under dendritic pattern indicate severe erosion hazards, where as those under trellis pattern indicate resistance nature of the rock strata.

Several tributaries, streams and drainage channels feed the river. Features of major tributaries are presented in table below (Table 3.4):

Table 3.4: Features of R. Dibang Joining Major Tributaries (up to Dam Axis)

River/Tributary	Reach	River Slope (% age)	Length of Rivers/ Tributary (km)
1. Ipui Nala (Right bank tributary)	Source to confluence Point with R. Mathun	6.2	22
2. R. Enzon (Left bank tributary)	Source to confluence Point with R. Mathun	5.3	41
3. R. Arun Chu (Right bank tributary)	Source to confluence Point with R. Mathun	5.9	31
4. R. Andra (Right bank tributary)	Source to confluence Point with R. Mathun	5.2	41
5. R. Elon Pani (Right bank tributary)	Source to confluence Point with R. Mathun	6.1	36
6. R. Dri (Left bank tributary)	Source to confluence Point with R. Dri (M)	4.3	56
7. R. Tangon (Left bank tributary)	Source to confluence Point with R. Tangon (M)	3.9	86
8. R. Emra (Right bank tributary)	Source to confluence Point with R. Tangon (M)	3.6	102
9. R. Ahi (Right bank tributary)	Source to confluence Point with R. Tangon/ Dibang	5.5	54
10. R. Ithun (Left bank tributary)	Source to confluence Point with R. Dibang	5.0	73
11. R. Imupani (Right bank tributary)	Source to confluence Point with R. Dibang	5.0	25
12. R. Ilupani (Right bank tributary)	Source to confluence Point with R. Dibang	5.2	24
13. Airi Nala (Left bank tributary)	Source to confluence Point with R. Dibang	2.2	0

3.3 METEOROLOGY

The Dibang basin falls partly in climatic zone I and partly in zone III. Zone I comprises of North and North Eastern part of India including Myanmar, Nepal, Bhutan, Bangladesh and part of Pakistan. Zone No. III comprises China, Tibet and portion of North and North Eastern part of Arunachal Pradesh. Climate in Zone No. I is generally tropical monsoon climate. Rainfall generally occurs during June to September in the monsoon period while the months of November to February are dry periods. Occasional rainfall occurs during May and October. The climatic Zone No. III can be classified as “Mountain Climate” because of atmospheric transparency isolation as mountains are stronger and richer in ultraviolet radiation than that at sea level. Mountain slopes exposed to the sun experience burning heat while slopes in shadow may be quite cold.

Two distinct climatic conditions prevail over the entire Dibang Catchment. The upper reach starts from the Indo-Tibet border up to Mayudiya Hill Range and the lower reach starts from Mayudiya Hill range to the confluence of Lohit. In the upper catchment, rainfall is comparatively less and the region is very cool during winter and comfortable during summer. The lower part maintains tropical climate. Rainfall is very high and the climate remains very humid.

3.3.1 Precipitation Characteristics

The rainfall in the basin is mainly influenced by the mountain system and occurs due to the Southwest monsoon, which sets in by the second week of May and continues upto the middle of October. On the basis of the available data, average rainfall in the basin upto the dam site has been estimated to be 4405 mm (Source: Feasibility report CWC 2003). However, the major portion of the rainfall occurs during the period from June to August. Station wise average rainfall in the basin is placed in table 3.1.

3.3.2 Precipitation Data network

Brahmaputra Board has installed twenty raingauge stations in the entire Dibang basin, out of which three stations have Self Recording Raingauge in addition to the ordinary type. Although a few stations have data w.e.f. 1985-86, most of the stations have data only from 1997 onwards. NHPC is also

installing ordinary/SRRG raingauge stations in Dibang basin. One ordinary and one SRRG station has already been installed at Munli near Dibang dam site and installation procedure of some more raingauge stations in Dibang basin is under process. The rainfall data availability status is given in table 3.5.

Table 3.5: Precipitation Data

Status of raingauge stations in Dibang basin as per Feasibility report CWC –2003 and Rainfall stations established by NHPC				
S.No.	Type of Data	Name of Station	Data available in NHPC	Source
1	Daily Rainfall	Ahralin	Jun 98 to May 2003	Brahmaputra Board
2	Daily Rainfall	Jiagaon	Aug 85 to Sep 87, Jan 89 to Dec 90, July 92 to Aug 93, Jan 94 to Dec 01, Apr 02 to Aug 02	Brahmaputra Board
3	Daily Rainfall	Elopa	Jun 97 to Jan 01, March, Apr, Aug to Dec 01, Apr 02 to Aug 02	Brahmaputra Board
4	Daily Rainfall	Ipingu	Apr 98 to Feb 2001, Aug 2001 to Dec 2001, Jan 2003 to May 2003	Brahmaputra Board
5	Daily Rainfall	Anelih	Aug 97 to Aug 2002	Brahmaputra Board
6	Daily Rainfall	Dunli	Sept 97 to Aug 2003	Brahmaputra Board
7	Daily Rainfall	Mipidam	Apr 98 to July 2001	Brahmaputra Board
8	Daily Rainfall	Kronli	Oct 85 to Dec 85	Brahmaputra Board
9	Daily Rainfall	Amarpur	Nil	Brahmaputra Board
10	Daily Rainfall	Anini	1979 to 1985, Feb 92 to Jun 95, 1999 to Aug 2003	Brahmaputra Board
11	Daily Rainfall	Agoline	Sept 85 to Apr 86	Brahmaputra Board
12	Daily Rainfall	Tangon	Sept 85 to Apr 86	Brahmaputra Board

13	Daily Rainfall	Epipani	Oct 85 to Oct 87, Jan 88 to Feb 88, Aug 88 to Jan 89, Sep 89 to Jun 90, Jan 91, Mar 94 to Nov 94, Jan 95 to Nov 95, Jan, Feb, May to Aug, Dec 96	Brahmaputra Board
14	Daily Rainfall	Chapakhowa	Sep 85 to Jul 86, Feb 87 to Nov 87, Jan 89 to Aug 90, Jan 91 to Jul 96	Brahmaputra Board
15	Daily Rainfall	Etalin	Aug 97 to May 2003	Brahmaputra Board
16	Daily Rainfall	Roing	1976 to 1981, 1985, Nov 84 to Aug 96, Jan 97 to Jun 2000, Oct 2000 to Mar 01, Aug to Dec 01	Brahmaputra Board
17	Daily Rainfall	Hunli	Sep 98 to Jul 2000, Nov 2000 to Dec 2000, Feb, Mar, Jun to Sep, Nov, Dec 01	Brahmaputra Board
18	Daily Rainfall	Christian Basti	Nil	Brahmaputra Board
19	Daily Rainfall	Nizamghat	Nil	Brahmaputra Board
20	Daily Rainfall	Munli	Jan-May 05	NHPC
21	SRRG	Hunli	Nil	Brahmaputra Board
22	SRRG	Roing	Nil	Brahmaputra Board
23	SRRG	Desali	Nil	Brahmaputra Board
24	SRRG	Munli	Mar 2005-May 2005	NHPC

3.3.3 Temperature

As per Prefeasibility report prepared by Brahmaputra Board March 2002 the meteorological observatory center in the Dibang basin is located in Hunli and Elopa. Temperature and Relative humidity data are collected here since 1998. The monthly maximum and minimum temperature and humidity recorded since September 1998 to June 2000 are given in tables 3.6 and 3.7.

Table 3.6: Observed Temperature and humidity data at Hunli

Month/year	Temperature maximum in C	Temperature minimum in C	Relative humidity Maximum in %	Relative humidity Minimum in %
September-98	26	10	92	81
October-98	24	6	91	80
November-98	19	4	90	76
December-98	17	3	88	68
January-99	16	2	88	66
February-99	14	2	89	75
March-99	18	7	89	75
April-99	19	9	89	75
May-99	25	12	91	89
June-99	27	16	91	81
July-99	30	17	92	74
August-99	29	16	92	82
September-99	27	11	91	61
October-99	22	11	89	64
November-99	16	8	88	52
December-99	12	7	87	71
January-00	14	7	88	71
February-00	19	8	89	49
March-00	20	12	90	59
April-00	33	14	92	34
May-00	30	19	92	82
June-00	31	18	92	78

Table 3.7: Observed Temperature and humidity data at Elopa

Month/year	Temperature maximum in C	Temperature minimum in C	Relative humidity Maximum in %	Relative humidity Minimum in %
June-98			92	76
July-98			92	84
August-98			92	92
September-98			92	85
October-98			93	83
November-98			92	76
December-98			92	65
January-99			91	71
February-99	30	19	92	41
March-99	37	17	92	42

April-99	32	17	91	44
May-99	39	20	92	49
June-99	39	22	92	52
July-99	39	20	92	52
August-99	37	22	92	70
September-99	37	23	92	70
October-99	36	20	92	61
November-99	32	17	92	53
December-99	28	13	89	19
January-00	26	13	91	20
February-00	28	14	89	34
March-00	35	16	85	51
April-00	35	16	85	51
May-00	37	21	92	53
June-00	39	23	92	49
July-00	31	18	92	48

NHPC is also establishing Automatic Weather Station (AWS) and Maximum Minimum temperature recording stations in Dibang basin. Out of these, one AWS/Maximum Minimum temperature recording station has been established at Munli w.e.f. March 2005. Some more stations may be established within few months.

3.3.4 Humidity

The relative humidity in the project area is high throughout the year. However, winter months are slightly less humid. The relative humidity ranges from a minimum of 19 % to a maximum of 92 %.

3.3.5 Cloud Cover

Clear or lightly clouded sky is common during the post-monsoon months. During winter season, the morning sky often remains overcast mainly due to lifted fog which gets cleared as the day advances. In the pre-monsoon months sky is generally moderately clouded. Heavily clouded to overcast sky prevails in the monsoon months, when hills and ridges are enveloped in cloud.

3.3.6 Wind

Winds are generally light during the south-west monsoon season. In rest of the year, winds are moderate, becoming strong at times in association with

thunder storms. Strong winds down the valleys are experienced. The direction of wind is highly influenced by the local conditions.

3.3.7 Special Weather Phenomena

Thunder storms mainly occur during the months from February to September. The frequency is maximum in April and minimum in the month of December. During the pre-monsoon months, thunder storms are often violent and from December to April they are occasionally accompanied by hail. Fog is frequent in the valleys during the winter months.

3.4 GEOLOGY OF THE RESERVOIR AREA

3.4.1 Bed Rock Geology

Regionally, the reservoir area lies at the junction of Eastern Himalayan mobile belt which terminate against N-W trending Parametamorphites and Diorite-Granodiorite Complex of *Mishmi block* in the Dibang Valley. The Eastern Himalayan mobile belt embodies a succession of northern dipping thrust sheets that occupy almost the whole of Arunachal Pradesh. The rocks of recent, tertiary and Paleozoic age are exposed which have undergone polyphases of deformation and metamorphism. Important tectonic elements falls in reservoir area are Tidding suture, Lohit thrust.

The main litho units exposed in the reservoir area (after Srivastava et.al, 1983-84) are:

- Ithun Formation
 - Hunli Formation
 - Ultramafics
 - Igneous Complex
- } Precambrian
- } Precambrian

3.4.1.1 Precambrian Meta-Sedimentaries

It consist of high grade biotite gneiss and garnetiferous mica schist termed as ***Ithun Formation*** and low grade chlorite schist with intercalations of phyllites and carbonate rocks termed as ***Hunli Formation***.

3.4.1.2 Ithun Formation

Ithun formation comprise of quartzofeldspathic gneiss, biotite gneiss, amphibolite, calcareous quartzite, carbonate bands and garnetiferous mica schist with kyanite and sillimanite. The general trend of these rocks is NW-SE with northeasterly dips. In the Ithun valley these rock unit forms the core of double plunging antiform with the axis along NW-SE parallel to the course of Ithun river. Biotite gneiss is the prominent rock of Ithun formation. It is fine to medium grained. Gneissosity is moderate to well developed and is defined by alternate micaceous and quartz-feldspar bands. In the Elopa-Annelih section, the Ithun formation is repeated due to folding. South of *Mrambon*, it shows an inverted disposition whereas to its north, the sequence is normal. The rocks of Ithun formation are co-relatable with mylonite granite gneiss of Pari-mountain Formation of Siang group and low grade interbanded sequence of quartzite, chlorite schist and marble of Siyom Group (*N. Srimal et al., 1998*). The rock units belonging to Ithun Formation constitute almost 50% of the reservoir rim.

3.4.1.3 Hunli Formation

The Hunli Formation consists predominantly of chlorite schist, quartz chlorite schist with green quartzite, phyllite, carbonaceous phyllite and carbonate rocks. All the above mentioned rock units show gradational contact with one another. Near the contact with the Ithun Formation, the rock are quartzitic and gneissic in nature. Characteristically, the quartz chlorite schist with quartzite in the contact zone gradually grades into the gneissic rock of Ithun formation. The rocks of Hunli Formation in Dibang valley are correlatable with near similar sequence of Tuting Meta-volcanics exposed around Tuting in Upper Siang district (*N. Srimal et al., 1998*)

The rocks of Hunli formation are well exposed in Echi-Nala area (South of Angolin), Etalin-Attunli section, at Ashu Pani-Dibang river confluence, Appako-Anelih section and Koroni area.

The rocks exposed in Etalin-Attunli section, Ashu Pani-Dibang confluence and at Koroni area shows an inverted sequence. Whereas the rock unit exposed in Echi-nala–Angolin, Appako-Anelih sections represented a normal sequence. The rocks show gradual steeping in dip amount towards the

Diorite-Granodiorite-Granite contact in *Echi-nala*. The rock units of Hunli formation contribute almost 30% of the reservoir rim. Incidentally, major landslide zones are located within Hunli formation.

3.4.1.4 Ultramafics

There are two major bodies of Ultramafics rocks. One is exposed in Myodia area along a synformal core with amphibolite and carbonaceous metapelites sequence, flanking on either side in Dibang valley inferred as the remnants of a tectonic slice (*N. Srimal et al., 1998*). The other occurs between the head of Ithun nala and Amilli village trending N-S and cutting across Ithun and Hunli formation (*Ray and Dutta, 1982*). Besides, there are several small occurrences in the area. Dunite, peridotite and pyroxenite are the dominant rock types.

3.4.1.5 Igneous Complex

A diorite-granodiorite-granite complex occur as a huge mass of batholithic dimension from Echi-nala to Maliyne and beyond in the Tangon Valley and extends westward along the Emra Valley. In Angolin area the diorite-granodiorite-granite shows sharp contact with biotite gneiss/schist and calcareous quartzite of the Ithun formation in the northern part of the body and its southern contact is faulted one with the Hunli formation. North of Echi-nala these rocks shows sharp contact with the meta-sedimentary rocks. The contact zone is characterized by feldspathisation and assimilation affects. These rocks would be coming almost at the tail end of reservoir.

3.4.2 Structure and Tectonics

In Dibang river valley, structural elements related to five phases of deformation are present. Each phase has produced folds with distinct characteristic geometry. First phase of folding (F1) is represented by tight isoclinal fold having schistosity or gneissosity as their axial planar structure. Second phase of folding (F2) is represented by moderately tight overturned folds defined by schistosity/gneissosity as well as bedding. Their axial planar structure is cleavage. These F1 & F2 folds are co-axial in nature. Third phase of folds (F3) are open type with NE-SW trends. Their axial plane is vertical

and defined by a prominent joint set. Fourth phase of folding (F4) is represented by NE-SW to NNE-SSW trending broad wraps having a prominent joint set as its axial planar structure. These trend across all the rock formations and hence considered as cross folds. Broad wraps along sub-horizontal axial plane having joint set as their axial planar structure represent fifth phase of folding (F5) that are of local importance.

Planar structures observed in the area are bedding, schistosity/gneissosity, cleavage, joint, shear and fault. Of these bedding is the only primary planar structure and the rest are secondary. Bedding is well developed in quartz-chlorite schist; carbonate rock and green quartzite of Hunli formation and quartzite of Ithun formation. Schistosity is well developed in chlorite schist and phyllite of Hunli Formation and gneissosity in gneissic rock of Ithun Formation

Following major thrust/faults are present in reservoir area:

- (i) Lohit Thrust – The diorite gneiss of Granitoid Complex are thrust above low grade meta sedimentaries of Hunli formation along northerly dipping Lohit thrust. The thrust zone is defined by shearing followed by re-crystallization of sheared rocks. It trends towards NW-SE with steep dips toward NE and suppose to merge with Yang Sang Chu Thrust in Siang Valley.
- (ii) Tidding Suture – With dismembered Ultramafic Suite marks the boundary between low grade sediments of Himalayan orogenic belt and moderately reworked meta sedimentary belt.

The evidence of neotectonic activities have also been recorded in the Dibang valley in the form of geomorphological and tectonic features, such as shear of local nature in tillite and clay sequence in Upper Dibang valley, presence of thick boulder zone sandwiched between sheared metadiorite and garnetiferous schist and presence of reverse faults within quaternary sand and pebbles.

In the reservoir area meta-sedimentary rocks of Ithun and Hunli formations are exposed as folded strata with the fold axis trending almost in NW-SE direction. In the upper reaches of the reservoir, granite-granodiorite rocks of Lohit igneous complex are present with thrust contact with meta-sedimentaries known as 'Lohit Thrust'.

A brief description of geology encountered along the main Dibang River and its major tributaries is described below:

(i) Geology of reservoir rim along Dibang river section

The rock exposure along the river banks, nala section, foot tracks were studied for reservoir mapping and it is noted that a variety of rocks belonging to different formations/groups are present. The litho units of the area are briefed hereunder.

In the reservoir area upstream of dam axis along the course of Dibang river and its tributaries viz *Ilu Pani* and *Ari Pani*, rocks of Ithun formation comprising of quartzo-feldspathic biotite gneiss, biotite amphibolite gneiss with bands of amphibolite chlorite schist are exposed. Upstream of *Ilu Pani* up to *Aounli* village several bands of quartzite (with schistose layers) having thickness of 100m to 500m are exposed along with gneiss. The rocks in this portion are intruded by several basic and ultra-basic dykes ranging in thickness between 2m to more than 50m.

Upstream of *Mrambon* village garnet content has gradually increased in the biotite amphibolite gneiss especially in the rocks exposed along the both banks of Dibang near *Attaya* village. Between *Ayyu Nala* and *Kronli*, biotite amphibolite gneiss grades into biotite schist/biotite chlorite schist/garnetiferous biotite schist etc., which is highly crumbled and sheared near *Allu nala* just downstream of *Kronli*. Few 60-70 m thick bands of calcareous quartzite are also exposed along the huge landslide developed in this area. Between *Kronli* and Ithun-Dibang confluence, mainly biotite chlorite gneiss/schist is exposed. Rocks of Hunli formation are exposed upstream of Ithun-Dibang confluence upto the *Echi-nala*, *Ahi* river valley and upstream. The rocks exposed along the road section in this portion are quartz-chlorite mica schist, graphite mica/schist with bands of carbonaceous rocks, chlorite

schist. In *Ikhi Pani* nala quartz-amphibolite schist is exposed. In *Echi-nala* the chlorite schist/graphite schist rocks grades into biotite-amphibolite schist of the Ithun formation which extends upto the Echi-nala.

Upstream of Angolin rocks of Lohit granodiorite complex comprising of quartz diorite, granodiorite, granite and luecogranite are exposed as we traverse northwards towards Etalin.

(ii) Geology of reservoir rim along Ahi River Section

The major rock type belonging to Hunli formation exposed in Ahi river section are quartzite gneiss with amphibolites and mica, graphite mica schist with occasional carbonaceous bands, crystalline limestone and quartz chlorite schist. The contact between these lithounits is gradational in nature. The quartzites show presence of amphibolites and mica with well developed gneissosity.



Photo 3.1: Feldspathic biotite gneiss outcrop on the left bank near cane-bridge, downstream of the confluence of Ichi nala with Dibang

Graphite mica schist is well exposed along *Ane Pani* nalla and along the Ahi River. It shows occurrence of several bands of carbonaceous rock. Limestone is exposed as 20-30m thick bands. The limestone is crystalline in nature, dark grey colored and fine grained. It has few phyllite intercalations. Chlorite mica

schist and graphite schist shows well developed schistosity. At the confluence of the Ahi river with Dibang, the quartz chlorite schist rocks gradually grades into feldspathic gneiss rocks showing steep dips (**Photo 3.1**). At the Ichi nala confluence feldspathic gneiss rock is exposed.

(iii) Geology of reservoir rim along Ithun River Section

In the Ithun river section rocks of both Hunli and Ithun formation are exposed. Quartz-chlorite schist and chlorite biotite schist with phyllites of Hunli formation are exposed upto Anaya village. These are intruded by several types of dykes and sills of basic and ultra basic nature. Upstream of Anaya village, amphibolite gneiss with intercalations of quartzite is exposed on both banks of Ithun.

3.4.2.1 Structures

In the reservoir area of Dibang, the meta-sedimentary rocks of Ithun and Hunli Formations generally trend NW-SE to E-W with steep to moderate dips towards north. These are deposited in an inverted manner as evidenced by the overlying nature of Ithun Formation and Hunli Formation and also by the occurrence of successive rock units of Ithun formation in its dip direction.

The Ithun and Hunli Formations are folded and faulted at several places. In Ahi river valley one major fault was observed near Alo Pani nala, resulting in offsetting of one phyllitic intercalation by 40m.

About 3 km downstream of Angolin quartz-diorite rocks of Lohit Granodiorite Complex abuts against biotite chlorite schist of Hunli formation as sharp contact. The highly disturbed nature of rocks, irregularity in foliations and exposure of basic intrusives near the contact shows presence of a major thrust. This is inferred as *Lohit Thrust*.

During course of reservoir mapping, several synclinal and anticlinal structures were observed. Chlorite mica schist exhibits one major anticline form about 1

km upstream of Ahi confluence on left bank of Dibang with graphite schist in the core of anticline. The fold axis plunges 30° towards 310° N.

Near *Aounli* village about 50 m thick shear/fracture zone was observed within biotite schist. This zone is NE-SW trending with moderate to steep dip towards NW direction.

3.5 LANDSLIDES

During the course of reservoir mapping of Dibang Hydroelectric Project several active and potential landslide along with other zones of mass movement were identified. However, prior to field traverse, a preliminary desk study was made to identify major unstable slopes utilizing IRS 1C/1D Geo-coded Satellite FCC's (False Color Composites) on 1:50,000 scale. These areas were cross checked in detail during field traverse and marked on the reservoir plan. A Digital Elevation Model (DEM) of the project area is also generated from State Remote Sensing Applications Centre, Itanagar to simulate and identify major landslide zones in the area. Following categories of unstable zones were identified within the reservoir area:

- (i) Ancient/passive slide debris cone covered with vegetation.
- (ii) Active landslide in overburden material.
- (iii) Active landslide in bedrock.
- (iv) Potential area of mass-movement and soil creep.

In the entire reservoir area overall 60 number of active landslide zones forming unstable slopes has been identified. These landslides are numbered from L-01 to L-60. The detailed description of these landslides along with their location, cause of sliding, type of failure etc. is described in **Table 3.9**.

These are further classified into small, medium and large categories based on their dimension and area (**Table: 3.8**):

Table 3.8: Categories and types of landslides encountered in the reservoir area of Dibang Multipurpose Project

Size of Landslide	Approximate area in m²	Approximate Dimension (width x height) (m²)	No of Landslides	Type of material
Small	Up to 1250	25 x 50	10	Mostly in overburden. Few in rock
Medium	1250 to 20,000	25 x 50 to 100 x 200	38	Both rock and overburden
Large	More than 20,000	More than 100 x 200	12	Rock in general

Most of larger landslides are developed in bedrock. However smaller and medium size landslides are observed in both rock and overburden cover along the proposed reservoir rim. It is observed that sliding in general has occurred due to plane/wedge failure along unstable slopes where foliation/joints are dipping steeply towards valley slope. Presence of major tectonic features in the area, surface runoff due to high precipitation and at places toe erosion by river channel are major factors that enhances the instability of the slopes in the reservoir area of Dibang. However, out of the above landslide zones only those landslides which are developed near the imminent periphery of the reservoir and comes in close proximity of the dam may have reasonable impact. The description of such major landslides that may have pronounced impact after the impoundment due to reservoir is given in the preceding paragraphs:

Table 3.9: Description of Landslides within the Reservoir Area of Dibang Multipurpose Project

S. No.	Landslide No. *	Location	Type of Failure	Cause of Failure	Vegetation	Slide material	Rock Type	Seepage
1	L-1	About 2 km u/s of Apruni village, on right bank of Dibang.	Plane failure along foliation plane.	Cross joints; Foliation plane cutting steep hill slope	No vegetation	Slide in rock	Biotite gneiss	No seepage
2	L-2	About 1.5 km d/s of Apruni village above road, on left bank of Dibang.	Plane failure along steeply dipping joint.	Fracture and closely jointed; weathered rock zone.	Sparse vegetation	Slide in rock	Granodiorite	No seepage
3	L-3	About 2 km d/s of Apruni village, on right bank of Dibang.	Circular failure, fan shaped structure found along nala.	Loose soil and seepage; Toe erosion by river.	No vegetation	Slide in overburden		Little seepage
4	L-4	About 250 m d/s of previous slide, right bank of Dibang.	Plane failure along steeply dipping joint.	Fracture and closely jointed; Toe erosion by river.	Sparse vegetation	Slide in rock	Granodiorite	No seepage
5	L-5	About 200 m d/s of previous slide, right bank of Dibang.	Plane failure along steeply dipping joint.	Fractured and closely jointed; Weathered rock zone.	No vegetation	Slide in rock	Granite / quartzite	No seepage
6	L-6	About 200 m u/s of Mayon river, on left bank.	Circular failure, up heavel observed at landslide toe.	Loose soil, toe erosion & high seepage.	Sparse vegetation	Slide in overburden		Seepage observed
7	L-7	About 500 m u/s of Emra-Dibang confluence, on right bank of Emra.	Wedge failure.	Criss cross joints; Joint plane intersecting steep hill slope.	Sparse vegetation	Slide in rock	Granodiorite	Seepage present
8	L-8	About 1.5 km u/s from confluence point, on right bank of Emra.	Plane and wedge failure; Several scarp faces are developed.	Cross joint; Sheared, fractured rock and weathered rock; Toe erosion.	No vegetation	Slide in rock	Granodiorite	Galleries seepage
9	L-9	About 1.8 km u/s from confluence point, on right bank of Emra.	Plane and wedge failure; Several scarp faces are developed.	Cross joint; Sheared, fractured rock and weathered rock; Toe erosion by river Emra.	No vegetation	Slide in rock	Granodiorite	Some seepage through temporary channels.
10	L-10	About 200 m u/s of Arhi nala, on right bank of Dibang river, d/s of Angolin village.	Plane and wedge failure; May be some thrust plane.	Criss cross joint; Joint plane cutting steep hill slopes, weathered rock.	No vegetation	Slide in rock	Granodiorite/quartz diorite	No seepage
11	L-11	On left bank of Dibang opposite to Arhi nala.	Plane failure.	Criss cross joint; Joint plane cutting steep hill slopes.	Partly vegetation	Base at road-cut, upper part in rock and lower part in overburden	Quartz diorite	Seepage through temporary channel.
12	L-12	On right bank of Enne nala.	Planer failure.	Criss cross joint; Weathered rock.	Partly vegetation	Slide in rock	Basic rock/Phyllite and schist	More seepage
13	L-13	On left bank of Dibang, d/s of Enne nala (Photograph 5.5).	Plane failure along steeply dipping joint planes; Several scarp faces are developed.	Criss cross joint; Weathered rock / litho contact; Joint plane cutting steep hill slopes; Extensive toe erosion by river Dibang.	No vegetation	Slide in rock	Calcareous quartzite/ phyllite + chlorite schist	No seepage
14	L-14	On left bank of Dibang, d/s of previous slide.	Plane and wedge failure; Several scarp faces are developed.	Several cross joint with high persistence, weak rock mass; Joint plane cutting steep hill slopes and toe erosion.	No vegetation	Slide in rock	Calcareous quartzite	No seepage
15	L-15	On left bank of Dibang, d/s of previous slide.	Plane and wedge failure; Several scarp faces are developed.	Closely fractured zone; Weathered rock zone; Steep joint plane cutting hill slope and toe erosion.	No vegetation	Slide in rock	Calcareous quartzite	No seepage
16	L-16	U/s of 173 km bridge, on right bank of Dibang.	Plane failure along foliation joints; Several scarp faces are developed.	Closely fractured zone; Weathered rock zone.	Partly vegetation	Slide in rock	Chlorite biotite schist	Few seepage gallery
17	L-17	On roadside, right bank of Echi nala.	Plane failure along the foliation plane.	Criss cross joint; Weathered rock; Sheared / fractured rock.	Partly vegetation	Slide in rock	Chlorite schist	No seepage
18	L-18	On roadside, right bank of Echi nala.	Plane failure along foliation plane.	Cross joints; Foliation plane cutting steep hill slope.	No vegetation	Slide in rock	Chlorite schist	No seepage

19	L-19	On roadside, right bank of Echi nala.	Plane failure along steeply dipping joint.	Fracture and closely jointed; weathered rock zone.	No vegetation	Slide in rock	Chlorite biotite schist	No seepage
20	L-20	On roadside, right bank of Echi nala, near bridge.	Plane failure along foliation joints.	Loose soil and seepage; Closely foliated and highly fractured joints; Criss-cross joints.	No vegetation	Slide in rock	Chlorite schist & calcareous quartzite	Few seepage gallery along the landslide
21	L-21	On roadside, left bank of Echi nala, near bridge.	Plane failure along steeply dipping joint; Several scarp faces are developed.	Fracture and closely jointed; Closely foliated rock.	Sparse vegetation at the base	Slide in rock	Chlorite biotite schist	Little seepage
22	L-22	Below road on left bank of Echi nala.	Plane failure along steeply dipping joint.	Fractured and closely jointed; Weathered rock zone.	Sparse vegetation at the base	Slide in rock	Chlorite schist	No seepage
23	L-23	Opposite to Echi nala confluence on right bank of Dibang.	Plane failure.	Closely jointed and foliated.	No vegetation	Slide in rock	Amphibolite gneiss	No seepage
24	L-24	On left bank of Chu nala.	Circular failure.	Loose soil and debris material.	Sparse vegetation	Slide in overburden		Few seepage galleries
25	L-25	On left bank of Chu nala, u/s of previous slide.	Plane failure.	Loose soil and debris material, toe erosion.	Sparse vegetation	Slide in overburden		Few seepage galleries
26	L-26	On right bank of Chu nala, u/s of previous slide.	Circular failure upheaved observed at landslide toe.	Loose soil, debris material and nala seepage.	No vegetation	Slide in overburden		Few seepage galleries
27	L-27	On right bank of Chu nala, opposite to L-25 slide.	Circular failure upheaved observed at landslide toe.	Loose soil, debris material and nala seepage.	No vegetation	Slide in overburden		Few seepage galleries
28	L-28	On right bank of Chu nala, d/s of L-25 slide.	Circular failure, upheaved observed at landslide toe.	Loose soil, debris material and nala seepage.	Sparse vegetation	Slide in overburden		Nala channels flow through the slides
29	L-29	On left bank of Dibang, d/s of bridge below Ardzo village.	Plane and wedge failure.	Criss cross joint; Weathered rock.	No vegetation	Slide in rock	Feldspathic-amphibole gneiss	No seepage
30	L-30	On right bank opposite to Pi nala.	Plane failure.	Criss cross joint; Weathered rock; Joint plane cutting steep hill slopes.	No vegetation	Slide in rock	Amphibolite gneiss	Few seepage channels
31	L-31	D/s of Ehre nala confluence with Dibang on left bank.	Plane and wedge failure; Several scarp faces are developed.	Several cross joint with high persistence; Joint plane cutting steep hill slopes.	No vegetation	Slide in rock	Amphibolite gneiss	Few seepage channels
32	L-32	On right bank of Dibang, opposite to Ikhi nala confluence.	Plane failure; Several scarp faces are developed.	Closely fractured zone; Weathered rock zone; Steep joint plane cutting slope.	Sparse vegetation	Slide in overburden		Few seepage channels
33	L-33	On right bank of Dibang, d/s of previous slide.	Plane and wedge failure; Several scarp faces are developed.	Closely fractured zone; Weathered rock zone.	No vegetation	Slide in overburden	Amphibolite gneiss	
34	L-34	On left bank of Dibang, d/s of Ehre nala.	Plane failure along the foliation plane.	Criss cross joint; Weathered rock; Sheared / fractured rock.		Slide in rock	Chlorite/ graphite schist	
35	L-35	On right bank of Ikhi Pani.	Plane type of failure along foliation plane; Wedge failure also observed.	Cross joints; Foliation plane cutting step hill slope.		Slide in rock	Quartz-chlorite-mica schist	
36	L-36	On right bank of Ikhi Pani, 1 km u/s of previous slide.	Plane failure along steeply dipping joint.	Fracture and closely jointed; weathered rock zone.		Slide in rock	Quartz-chlorite-mica schist	
37	L-37	On left bank of Ikhi Pani, opposite to L-35 slide.	Plane failure.	Criss-cross joints; Sheared / fractured rock.		Slide in rock	Quartz-chlorite-mica schist	
38	L-38	On left bank of Dibang, u/s of Ithun confluence.	Plane failure along steeply dipping joint; Several scarp faces are developed.	Fracture and closely jointed; Sheared schist bands.	No vegetation	Upper part in rock & lower part in overburden	Feldspathic-amphibolite gneiss	Little seepage

39	L-39	On left bank, d/s of Ithun-Dibang confluence. (Photograph 3.4)	Plane failure along steeply dipping joint.	Fractured and closely jointed; Weathered rock zone and schist band; Extensive toe erosion by river Dibang.	No vegetation	Slide in rock	Amphibolite gneiss	Little seepage
40	L-40	On left bank, tributary of Ithun near confluence with Dibang river.	Plane failure.	Criss-cross joints; Weathered rock zone.	No vegetation	Slide in rock	Amphibolite gneiss	Little seepage
41	L-41	On left bank of Ithun, 2.0km u/s of previous slide.	Wedge failure.	Criss cross joints; Joint plane cutting steep hill slope.		Slide in rock	Quartz-chlorite schist	
42	L-42	On left bank of Ithun, 500 m u/s of previous slide.	Plane and wedge failure; Several scarp faces are developed.	Cross joint; Sheared, fractured rock and weathered rock.	Vegetation present	Lower part in rock & upper part in overburden	Feldspathic-amphibolite gneiss	
43	L-43	On left bank of Ithun, 1.5km u/s of previous slide.	Wedge failure; Several scarp faces are developed.	Cross joint; Sheared, fractured rock and weathered rock.		Slide in rock	Amphibolite gneiss	
44	L-44	On left bank of Ithun, 2km d/s of Ithu nala.	Plane and wedge failure.	Criss cross joint; Joint plane cutting steep hill slopes, weathered rock.	Covered with grass	Slide in overburden	Amphibolite gneiss	
45	L-45	On right bank of Ithun, d/s of Thi nala.	Plane and wedge failure.	Criss cross joint; Joint plane cutting steep hill slopes.		Slide in rock	Amphibolite gneiss	
46	L-46	On left bank of Ithun, u/s of Ithu nala.	Plane and wedge failure.	Criss cross joint; Weathered rock.	Covered with grass	Slide in rock	Amphibolite gneiss	
47	L-47	On right bank of Ithun, u/s of Shukla nagar.	Plane and wedge failure.	Criss cross joint; Weathered rock; Joint plane cutting steep hill slopes.	No vegetation	Slide in rock	Biotite gneiss	Little seepage
48	L-48	On left bank of Ithun, 128m d/s of Ithun bridge.	Plane and wedge failure; Several scarp faces are developed.	Several cross joint with high persistence; Joint plane cutting steep hill slopes.	No vegetation	Slide in rock	Amphibolite biotite gneiss	Little seepage
49	L-49	On left bank of Ithun, u/s of previous slide.	Plane failure in debris noticed.	Loose debris material.	Vegetation present	Slide in overburden		Few seepage galleries.
50	L-50	On right bank of Ithun, u/s of previous slide.	Plane and wedge failure; Several scarp faces are developed.	Closely fractured zone; Weathered rock zone.		Slide in rock	Chlorite schist	
51	L-51	On left bank of Dibang, d/s of Kronli village. (Photograph 3.3)	Plane failure along the foliation plane; Some tectonic lineament appear to pass from this slide zone.	Criss cross joint; Weathered rock; Sheared / fractured rock; Lithological contact and sheared schist bands.	Sparse vegetation	Slide in rock	Amphibolite gneiss & biotite schist	Little seepage
52	L-52	On left bank of Dibang, u/s of Akka nala confluence.	Planer type of failure along foliation plane.	Cross joints; Foliation plane cutting steep hill slope.		Slide in rock	Feldspathic-amphibolite gneiss	No seepage
53	L-53	On left bank of Dibang, u/s of Itti confluence.	Plane failure along steeply dipping joint.	Fracture and closely jointed; weathered rock zone.	No vegetation	Slide in rock	Quartzite	No seepage
54	L-54	On right bank of Dibang, u/s of Aouli village.	Plane and wedge failure.	Criss-cross joint; Closely jointed.	No vegetation	Slide in rock	Feldspathic-amphibolite gneiss	Little seepage
55	L-55	On right bank of Dibang, u/s of Aouli village.	Plane failure along steeply dipping joint.	Fracture and closely jointed.	No vegetation	Slide in rock	Feldspathic-amphibolite gneiss	Little seepage
56	L-56	On right bank of Dibang, 2.3 km u/s of Illu confluence (near to sharp band).	Plane failure along steeply dipping joint.	Fractured and closely jointed; Weathered rock zone.	Sparse vegetation	Slide in rock	Feldspathic-amphibolite gneiss	Little seepage
57	L-57	On left bank of Dibang, 500 m d/s of previous slide.	Wedge failure.	Closely jointed and foliated.	Sparse vegetation	Slide in rock	Feldspathic-amphibolite gneiss	Little seepage
58	L-58	On right bank of Dibang, 500 m d/s of previous slide.	Wedge failure.	Criss cross joints; Joint plane cutting steep hill slope.	Sparse vegetation	Slide in rock	Feldspathic-amphibolite gneiss	Little seepage
59	L-59	On left bank of Dibang, d/s of Illu Pani confluence.	Planer and wedge failure; Several scarp faces are developed.	Cross joint; Sheared, fractured rock and weathered rock.	No vegetation	Slide in debris	Feldspathic gneiss	No seepage

60	L-60	On right bank of Ari Pani (Photograph 3.2).	Planer and wedge failure; Several scarp faces are developed.	Cross joint; Sheared, fractured rock and weathered rock.	No vegetation	Slide in rock	Amphibolite gneiss	No seepage
61	L-61 +	On left bank of Dibang, between Munli-Ashu Pani confluence.	Planer and wedge failure.	Criss cross joint; Joint plane cutting steep hill slopes, weathered rock.	No vegetation	Slide in rock	Feldspathic gneiss	No seepage
62	L-62 +	On left bank of Dibang, u/s of Ashu Pani confluence (d/s of previous slide).	Planer and wedge failure.	Criss cross joint; Joint plane cutting steep hill slopes.	No vegetation	Slide in rock	Amphibolite gneiss	Nala present

Note:- (i) * For landslide number and location refer to Geological maps of the reservoir area on 1:15,000 scale.
(ii) + Landslides no. L-61 and L-62 are present downstream of the dam axis on left bank.

As we traverse upstream of the dam area, one major active landslide is present near the confluence of Ari Pani nala with Dibang about 2 km upstream of proposed dam axis (**Photo: 3.2**). This slide has taken place in sheared feldspathic gneiss rock and extends for about 500m above bed level with 150 m width at the base. The slide is active and is formed mainly due to failure along weak shear seams and joint planes which coincides with the steep hill slope. This landslide is indicated as L-60.



Photo 3.2: Active landslide zone near Airi Pani confluence with Dibang river (about 2 km u/s of Dam axis)

Other major landslide zone is present on left bank of Dibang downstream of Kronli village and is identified L-51 (**Photo: 3.3**). This massive landslide extends for about 900 m from river bed up to its crown and has a lateral extent of about 800m at the base. This area marks highly disturb zone and anticipated to be associated with tectonic lineament as evident by highly crushed and sheared mica chlorite schist and gneissic rocks of Hunli formation present in this area. Several steeply to moderately sloping scarp faces are exposed along the slide. This slide zone is highly active especially during the monsoon season when surface runoff and seepage is enormous. The frequency of sliding has enhanced during the last 15 years due to which entire Kronli village has been evacuated and resettled at Ardzoo.



Photo 3.3: Active landslide zone (more than 1.5 km in extent) downstream of Kronli in the rocks of Hunli Formation



Photo 3.4: Active landslide zone, left bank of Dibang at the confluence of Ithun and Dibang river

The landslide present at the confluence of Ithun and Dibang river on the left bank is indicated as L-39. This slide is also active in nature (**Photo: 3.4**). It extends up to 500 m elevation from river bed and is about 200 m wide at base. This slide has occurred in amphibolite gneiss/schist which is intruded by several basic dykes. The slide is formed due to planar and wedge failure along the steep hill slopes. High rate of toe erosion by Dibang river is also a major contributory factor. Another major landslide zone indicated as Slide no. L-13 is present about 1.2 km downstream of Enne nala (**Photo: 3.5**). It is formed as a result of planar failure along steeply dipping beds of calcareous quartzite and mica chlorite schist of Hunli formation. High rate of toe erosion and presence of steep valley slope are other contributory factors.

The other large landslide zones are located in the upstream reaches of the reservoir; many of them are at higher elevations in various tributaries of Dibang and may not pose much threat. Rests of the landslides are medium to small in nature and will have not much impact on reservoir stability. The major landslides will require further studies during pre-construction stage to evolve suitable remedial measures.



Photo 3.5: Landslides on left bank of Dibang about 1.2 km downstream of Enne nala. High rate of toe erosion and failure along weak planes has made this slide active

3.6 SEISMOLOGY

The North Eastern Region of India and its environment are both tectonically as well as seismically very dynamic and active. This region has been a source of two of the greatest earthquakes in the world with magnitude greater than 8.5, besides which, several earthquakes of magnitude 7.0 and more occurred in the region. Some of the modern day destructive earthquakes that have occurred in this region are of 1869 (M=7.5), 1875, 1897 (M=8.7), 1918 (M=7.6), 1930 (M=7.1), 1943 (M=7.2), 1950 (M=8.7), 1957 (M=7.2), 1984 (M=5.5), 1988 (M=7.3) and 1997 (M=5.3). On the basis of past recorded earthquakes, various scientists have predicted a due for high magnitude earthquake from this region (M>7.0). Whatever may be the time and place for such predicted high magnitude earthquake, yet, intermittent release of energy through micro to macro earthquake from this region are taking place throughout the year. Since the earthquakes are great natural hazard, it has become imperative to study seismic hazard for all developmental projects and to minimize it.

3.6.1 Tectono-Stratigraphic Set up

Regional tectonics and seismic history of the North Eastern Region is highly significant. It constitutes active, unparallel relief, complex geological set up and anomalous crustal structure, which are attributed to the direct collision between Indian plate (Himalaya) and China / Tibet plate in the north and Indo-Burma subduction plate tectonics in the south east. This continent collision and subduction tectonics has developed juxtaposition of three tectonic blocks, viz N.E. projection of Indian shield with Himalayan thrust front, Eastern syntaxis of Mishimi block and the thrust imbricated Indo-Burmese block as well as the intervening Brahmaputra and Surma Valley.

In the Himalayan belt, a few well defined techno geologic domains extend over a distance of 2500 km from Nanga Parbat in the west to Namcha-Barwa in the east. In the north of Arunachal Himalaya, the southern margin of Eurasian plate is marked by Indus Tsangpo Suture Zone (ITZ). The 15 to 20 km wide Tsangpo ophiolite melange occurs along the Tsangpo river course and extend beyond the Siang fracture and the serpentinites of Mishimi block occurring in association with actinolite tremolite schists as well as crystalline

limestone. The diorite-granodiorite complex of Mishimi block is thrust over the frontal metamorphics, consisting of high to low grade metamorphic rocks with serpentinites along the NW Lohit thrust. The metamorphics in turn override the Neogene folded rocks of the Burmese arc by the Mishimi thrust in Noa Dihing Valley.

The highest axial zone of Himalaya is occupied by the Proterozoic crystalline rocks delimited to the south by the Main Central Thrust (MCT). The Neogene granites are common along the contact of the crystallines and the Tethyan sediments. The well-defined Lesser Himalayan belt between MCT and MBT, in all probability, may represent the tectonised northern extension of the Indian shield with both fresh water and marine sediments and orthoquartzite-dolomite sequence. South of the MBT, all along the foot hills, occur the folded and thrust belt of Upper Tertiary molassic Siwalik sediments with slices of Gondwana and Eocene rocks at some places. South of the Siwalik belt is the Brahmaputra alluvial plain.

The Meghalaya plateau and Mikir hills consisting mostly of Archean gneissic complex and Proterozoic intercratonic sediments of Shillong Group intruded by Upper Proterozoic granite batholith and basic igneous rocks, represents a positive shield element. This block occupies a crucial position between the Himalaya in the north and North West and Burmese arc in the east and south east. The Dauki fault at the southern margin of the plateau separates it from the Sylhet plain of Surma Basin. Cretaceous Tertiary shelf sediments occur along the southern margin of the plateau. The Upper Assam Valley forms a fore deep for the Himalaya and the Burmese arc.

The Naga Patkoi belt is composed of thick sediments of Eocene flysch, coal bearing Barails, uncomfortably overlain by middle and upper Tertiary rocks consisting of sandstone, clay shale and pebble beds. The ultra basic ophiolites occur along Indo- Burmese border. The belt of schuppen consists of several thrust slices, viz Haflong thrust, Disang thrust, Margherita thrust, Naga thrust, are some prominent features, which are mostly over thrust with some overlap.

3.6.2 Tectonic Setting

In the figure 3.1 generalized Tectonic map of North East India is shown. The East West structural trend of the Himalaya has- taken a sharp bend towards North East - North in the Siang Valley, Arunachal Pradesh. The available geological information do not indicate physical continuity of the Himalayan rock units across the Siang fracture (Nandy, 1980) into the Mishimi block, rather the north east trending elements of Arunachal Himalaya with its thrust sheets abut against the north-west trending structural grain of the Mishimi block. The MGT and the MBT are the two major crustal discontinuity extending west to east through out Himalaya, but these do not represent single dislocation plane. The MBT is well exposed all along the southern margin of Arunachal Himalaya upto Siang river, while MCT is yet doubtful about its extension. Thrusting along the MBT is a late event involving the youngest Siwalik rocks of Pliocene to Pleistocene age. Besides these longitudinal thrusts / faults, many oblique to transverse faults lineaments cut across the Himalaya, some of which are regionally extensive and traverse from fore deep to ITZ through Himalaya. Few of these caused noticeable off sets on MBT & MCT in the Siang fracture zone.

The most prominent and significant tectonic feature around the project site are apparently parallel NW trending Mishimi thrust and Lohit Thrust. This tectonic block over rides the NW and SE dipping thrust packets of Himalaya and Burmese arc, respectively. The northern boundary of this block is Po Chu Fault. The frontal Mishimi thrust in this zone show late Neogene thrusting over the Upper Assam alluvial plain while recent seismic activity indicates predominant right lateral shear.

Amongst the N-S trending fault, Bame fault has affected other tectonic features in Arunachal Himalaya. Bame fault is connected with the Eastern syntaxis and appears to be related to the refolding of rocks due to collision of Burmese plate with the Indian plate during Post Lower Eocene time.

The Great Assam Earthquake of 1950 ($M=8.7$), originating from this domain, illustrates similar right lateral sense of displacement (Ben-Menahem et al, 1974). The southern corner of this domain is at present most active where ENE thrust sheets of Burmese arc intersects the NW Mishimi and Lohit thrust.

In addition to the above tectonic lineaments of Arunachal Pradesh, other regionally extended prominent tectonic features of the region are:

- a) Dauki fault in the south of Shillong plateau separating Shillong massif from the Surma basin of Bangladesh.
- b) NE trending Sylhet fault extending from Bangladesh and merging with Haflong Disang fault.
- c) N-S trending Jamuna fault demarcating western boundary of Shillong plateau from the Rajmahal gap.
- d) Hidden, conjugate Brahmaputra lineament.
- e) N-S trending Chidrang, Oudhnai, Krishnai, Kulsi, Kopili fault.

3.6.3 Seismicity of the Region

The study of distribution of all available earthquake epicenters of the region shows that the dispersion is not uniform in space. However, close view reveals that some of the epicenters do not follow major lineaments in true sense. But considering cut off magnitude and accuracy of data acquisition, some correlation can be made with probable source. In a very generalized way epicenter clustering can be visualized around (1) Western part of Shillong Plateau, (2) Central Assam & Western Arunachal Pradesh, (3) Indo Burma Border, and (4) North Eastern part of Arunachal Pradesh. The Upper Assam Valley area show less epicenter distribution, which was designated as Assam Gap area by Khattri (1987). Further, in this gap area only a few small magnitudes of earthquakes have generated. But it is established that this area is in fact a seismic and not a seismic gap area.

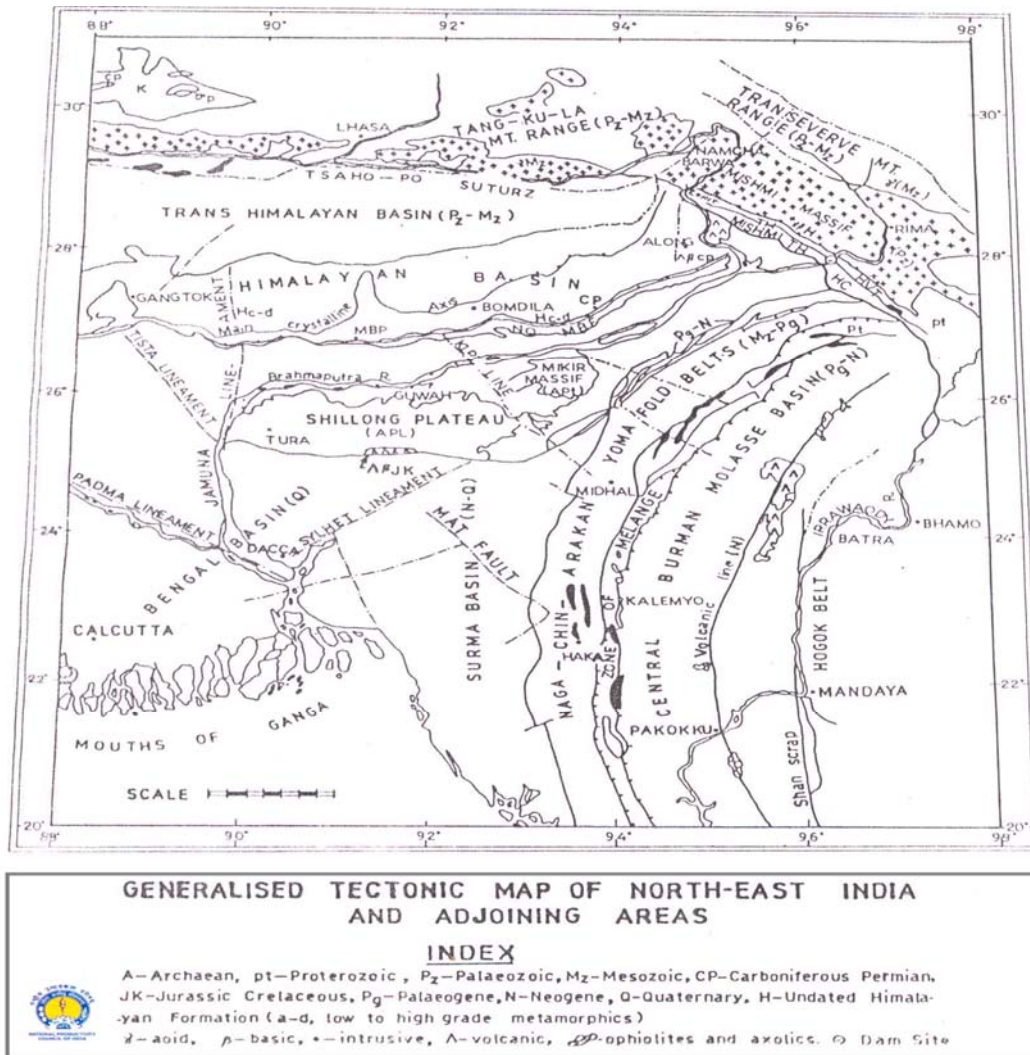


Figure 3.1: Tectonic Map of North East

The epicenter map considering ISC data source and 84 reliable shallow events of $M \geq 4.9$ for a period of 1963-84 along with recorded events ($M \geq 7.0$) of pre 1963, when superimposed on a tectonic map revealed the following.

- In the north of Suture Zone only a few seismic events are located.
- Seismic events are mostly located between MBT & MCT in the lesser Himalaya domain.
- Earthquakes occurring between MBT & MCT are evenly distributed along the Himalayan front and tend to concentrate in areas traversed by fractures/ faults across the strike of the Himalaya.
- The Upper Assam Valley in between the Himalayan front and the belt of Schuppen is largely aseismic upto the Mishimi thrust.

- e) The Mikir Hills & Meghalaya Massif has witnessed a few moderate events.
- f) The Sylhet plains, south of Dauki fault and the Mishimi block are more active relative to their immediate surroundings.
- g) The Assam earthquakes ($M > \text{ or } = 7.0$) of 1897, 1930 (Dhuburi) and 1943 (Kopili) are all located south of the Himalayan thrust front.
- h) The Great Assam earthquake of 1950 ($M=8.7$) located within Mishimi tectonic block that has been caused by the displacement along an inclined fault lying across the Assam axial belt trending NE-SW direction (Ray, 1953).

From the study of seismicity and tectonics of the region, the following active seismotectonic domains that have bearing on the construction of projects in the region, have been visualized.

- a) Mishimi tectonic domain,
- b) Kopili Bomdila tectonic domain (Himalayan), c) Sylhet tectonic domain,
- d) Indo Burma plate tectonic domain, and
- e) Shillong plateau domain.

The Seismotectonic Map of the area around the project site is shown in figure 3.1. The proposed project lies in the junction of Himalayan tectonic and Mishimi tectonic domain, more specifically the project site lies between active Mishimi thrust and Lohit thrust trending & paralleling in NW-SE direction with North Easterly dipping. 24 number of earthquake epicentres lie on the east of the thrust, 16 between the two thrust and 10 to 15 in the south of the Mishimi thrust.

3.6.4 Stress Distribution / Fault Plane Solution

Some of the published fault plane solution indicating stress mechanism of the fault during the event from this Mishimi Tectonic domain and around the project site, are tabulated below (Table 3.10):

Table 3.10: Parameters of Fault Plane Solution Earthquakes

Sl. No.	Date	Lat. N (deg)	Long. E (deg.)	Depth (km)	Magnitude
1	28.11.84	26.65	97.08	15	5.7
2	12.08.76	26.70	97.04	31	6.2
3	10.03.70	26.83	96.98	24	5.2
4	21.11.79	27.10	97.04	42	5.5
5	25.04.79	27.43	96.63	23	4.9
6	20.01.84	28.65	96.36	26	5.0
7	01.03.83	28.63	96.05	27	5.1
8	06.12.79	30.00	95.48	22	5.2
9	22.04.82	29.94	95.00	14	5.0
10	14.03.67	28.41	94.29	20	5.7
BM1	15.08.50	28.50	96.70	-	8.7

Sl No.	P-Axis		T-Axis		B-Axis		Nodal Plane 1			Nodal Plane 2		
	P1	Az	P1	Az	P1	Az	S	D	DD	S	D	D
1	04	284	35	16	54	187	N54W	63	144	N24W	69	249
2	40	108	24	357	40	244	N56E	80	326	N44W	42	224
3	10	111	05	202	78	310	N66E	80	336	N24W	86	246
4	28	187	47	64	31	296	N58W	80	212	N48E	34	318
5	36	178	06	84	53	346	N44W	70	46	N34E	60	304
6	25	268	16	5	58	124	N45W	84	45	N48E	60	118
7	10	270	05	N	80	110	N46W	85	44	N45E	80	115
8	47	190	06	94	44	1	N30W	64	60	N41E	55	311
9	03	178	42	252	48	81	N54W	60	36	N52E	63	142
10	01	75	30	45	60	167	N56W	70	215	N26E	70	116
BM 1	19	193	22	291	60	157	N26W	60	64	N52E	88	152

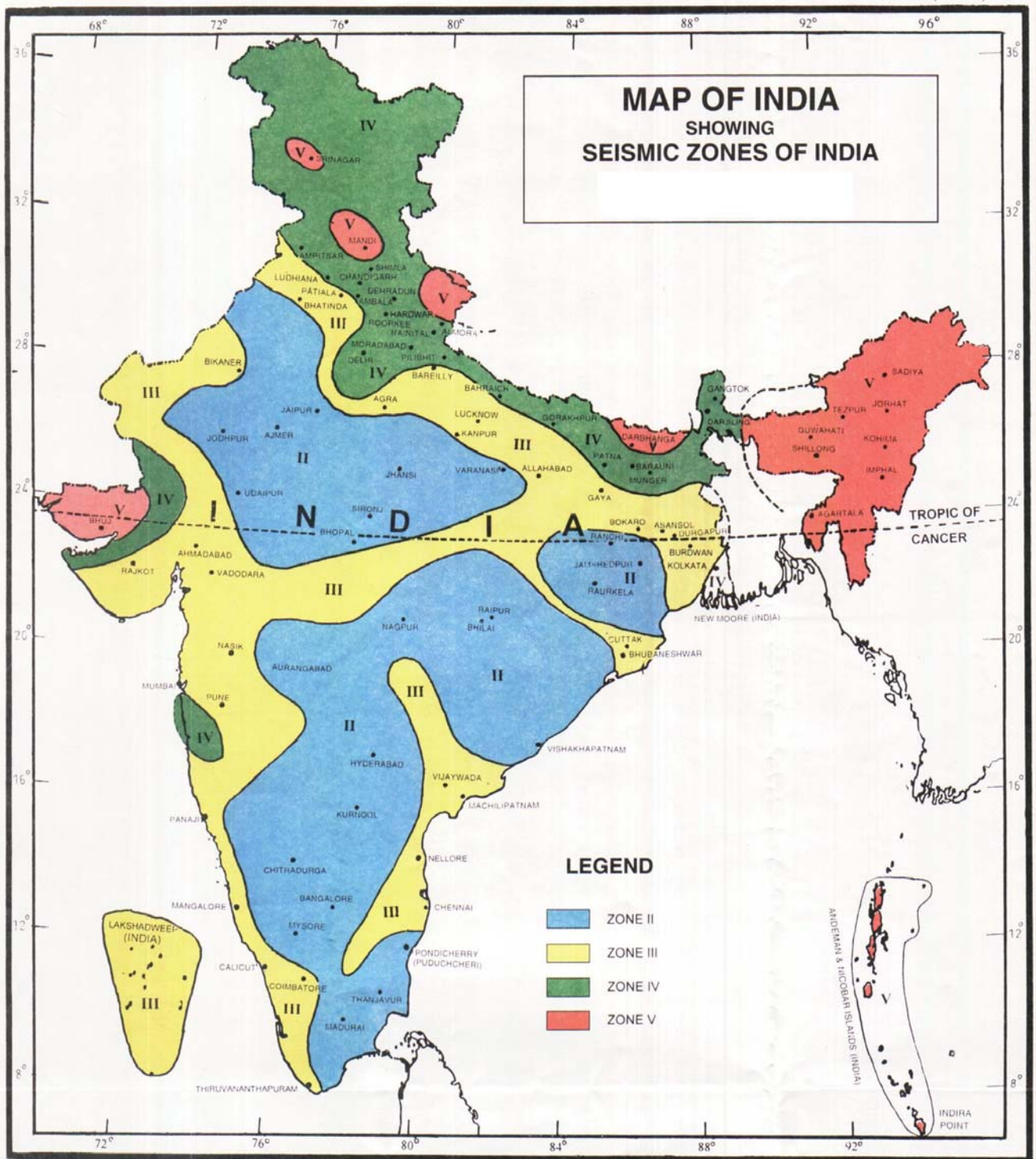
Ben-Menahem , et ai, 1974

The earthquake events at Sl. no. 1 to 3 are located within the ENE trending thrust zone (Margherita thrust Disang thrust) at the extreme northern boundary of Burmese arc and near the intersection with Mishimi Block. These three solutions suggests right lateral strike slip faulting along steeply dipping NE to ENE nodal planes. The solution of events 4 & 5 are located on Mishimi thrust with right lateral shear along NW trending nodal planes. Events 6 & 7 lie well within the Mishimi block and show sinistral displacement along NW fault plane. Solution of 1950 Great Assam Earthquake given by Ben - Menahem (1974) located along Po - Chu Fault zone indicates dextral slip along NW

nodal plane and rupture took place with velocity 3 km/sec on fault length of 250 km with 80 km width striking 330° - 337° and dipping 60° on ENE (64°). However, Chen & Molnar (1977) suggested thrust solution for the same events.

In the north west of Mishimi Domain, the MCT shows some activity as revealed from event no. 10 & 11 suggesting thrust type solution given by Fitch (1970) and Molnar et al (1973). However; recent solution by Nandy and Dasgupta indicate left lateral displacement for event 10 and dextral shear for event no. 11 along NW nodal plane.

Summarising the analysis of seismicity and stress distribution pattern of the area around the project site, it can be concluded that the zone of intersection of Mishimi block and the northern part of Indo Burmese arc reveals a complex geo-dynamic setting. The area is highly seismic and energy is released by dextral motion along ENE fault. But the seismic activity in the Mishimi block proper, suggest both NW dextral and sinistral displacement. Geological evidence (Nandy, 1980) however indicate that the outer most element of the Mishimi block moves towards the south west over the Pleistocene boulder bed. Further, the Upper Assam valley is observed to be aseismic.



Map 3.8: Seismo-tectonic Map of India

3.6.5 Seismic Risk

The proposed hydroelectric project is located within the Mishimi tectonic domain between two active thrusts. More precisely, the site falls within a

trifaceted tectonic platform, morpho-tectonically representing a 'structural knot' as recognized by Bhatia et al (1992). This structural knot has formed by two parallel longitudinal (1st order), two transverses (IInd order) and NS (IIIrd order) morphostructural lineaments and recognized as seismically potential zone for earthquake of $M \geq 6.5$ or 7.0.

The earthquake epicentre map of NEI (figure 3.3) reveals that the area around the project site is a potential source of seismic event. The Great Assam Earthquake of 1950 ($M > 8.5$) has occurred within 50 km radius, while number of major earthquakes $7.0 < M < 8.0$ have occurred within 100 km radius of the project site.

Besides, a number of events of $5.0 < M < 6.0$ occurred around the proposed project site. The area has experienced highest intensity being of the order of IX to X during 1950 Great Assam Earthquake. Due to this earthquake, Dibang river, along with other tributaries were blocked by landslides. During the Assam Earthquake of 1897, this area experienced intensity of the order VIII on mm scale. Further, as per Earthquake Zoning map of India this area falls within Zone V (Map 3.8).

On the basis of above experience it is believed that ground shaking could cause heavy damage during an earthquake. In this context for estimating actual level of damage to the structures, the Peak Ground Acceleration (PGA) should be taken into consideration. Considering NOM catalogue of seismic data and using probabilistic hazard assessment, the PGA for 10 % probability of exceedence in 50 years has been estimated to be 0.25 g for North Indian plate boundary region and Tibetan plateau region, while the North Eastern India and Burmese arc have been considered as highest risk zone with PGA value of the order of 0.35g to 0.40g (Kumar and Bhatia, 1991). However, considering the highest magnitude earthquake of 8.7 around the project site and tectonically being most complex site, the actual PGA need to be re-evaluated, although elsewhere 0.23g has been suggested for engineering structures in this area. (Ram Chandra, Pradhan and Dhanota, 1981).

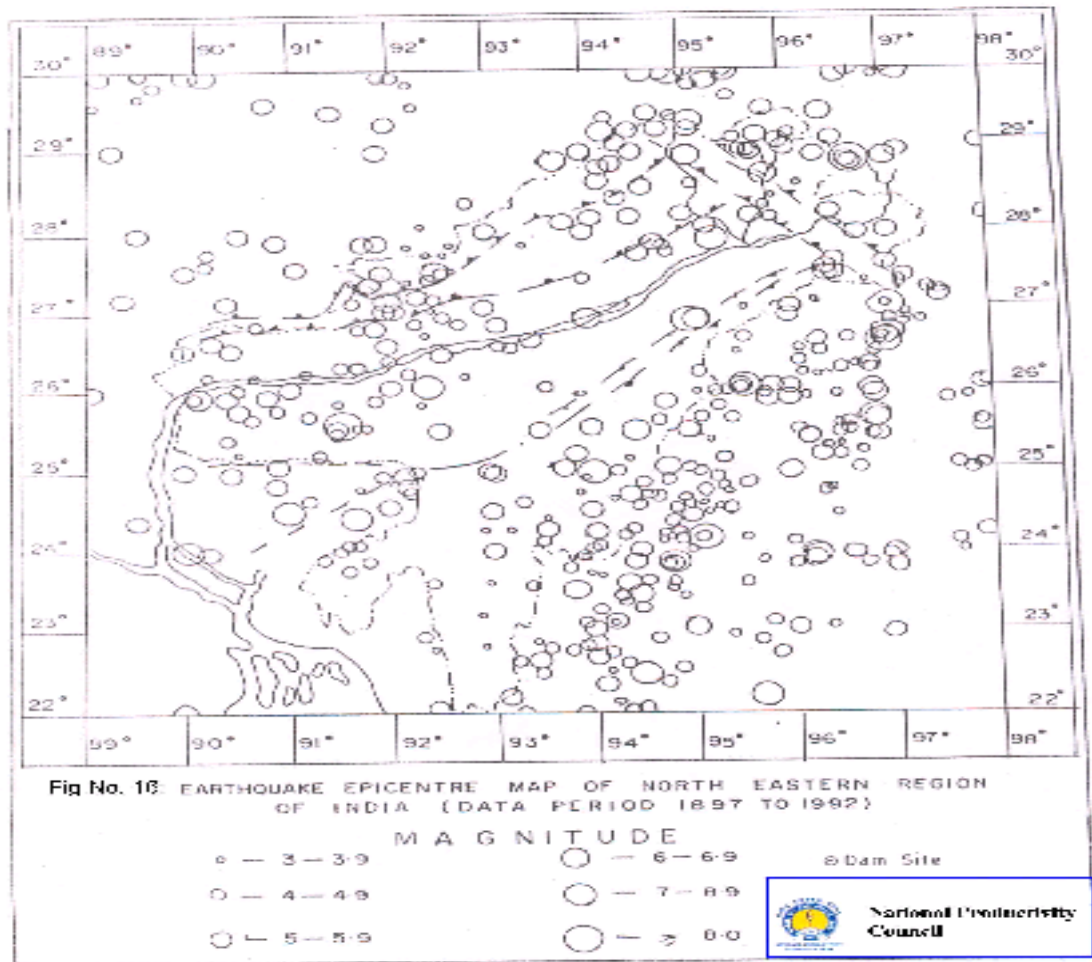


Figure 3.2: Earthquake epicentre

3.6.6 Reservoir Induced Seismicity

With the increase in developmental activities, like artificially impounding of lakes for hydropower generation, documentation of Reservoir Induced Seismicity (RIS) in the world has increased. Hence, for mitigation of such RIS hazard, it is necessary to pay special attention for individual sites.

In the Himalayan terrain, some of the artificial reservoirs have water column more than 100 m and reservoir volume more than 10^9 m^3 . In recent past, it has been emphasized by Gupta et al (1986) that besides normal high seismicity, the effect of such local reservoir on local seismicity is of great concern in and around the reservoir. As the proposed reservoir would be situated in high natural seismic domain with maximum probable magnitude =8.0, $\text{Nu} = 0.426$ and $\text{Beta} = 0.997$ (after Kumar and Bhatia, 1999), 'A' Value = 4.02, and 'b' value = 0.670 (after Sharma, 1999), it is essential to study the

seismic status of both natural seismicity) and RIS status of the area in detail. Although RIS incidence causing severe threat to any such structure within the Himalayan domain is not much reported, yet, the probability can not be ruled out without proper study of seismic and seismotectonic status of the site through monitoring of both pre and post impounding stages. Further, there is hardly a few reservoir within the Himalayan tectonic domain having adequate instrumentation for seismic surveillance. The record of non-occurrence of RIS has been attributed mainly due to thrust fault environment usually prevalent in the Himalayan foothills.

The dominant fault environment plays significant role in generating RIS. The focal mechanism, solution for earthquake in the nearby project site indicate mostly thrust and strike slip movement. RIS is generally noticed in low to moderate seismic areas. In highly seismic areas like this project, the normal stress changes may be larger than the incremental changes caused by impounding, hence induced seismicity may only cause changes in the frequency pattern of the natural seismicity.

As mitigation measures, a specific impounding rate may be called for in the design. Further, impounding should be smooth. RIS is generally observed within a few years of impounding, hence, it is recommended that the reservoir, as far as possible, should not be exploited in the initial few years. Exploitation brings down the level and results in high rate of impounding subsequently.

Considering the generalized tectonic setup of the project site, the RIS may have little effect and significance in view of : a) high seismic background nature, b) transverse normal fault environment within the project site, while the E-W trending thrust and strike slip will not have much bearing on the reservoir. However, the status of NW trending Mishimi thrust and Lohit thrust need thorough study.

The ponding of this reservoir falls under high reservoir, being 245.0 m height. According to Stuart and Alexander and Mark, chances of RIS occurrence of such high ponding cannot be ruled out. Further, reservoir located on hard rocks, which are comparatively impervious to seepage are prone to RIS factor than those located on weaker rocks which are porous. Later, physical condition of the impounding basement media perhaps safeguards the rock stability. The proposed reservoir falls within both hard and soft media base

rock. However, thorough geological mapping of catchments area is highly warranted.

3.7 WATER QUALITY

The Dibang river basin has low population density, with low irrigation intensity. In addition, there are no major sources of organic pollution also in the catchment area intercepted till the dam site. The low cropping intensity coupled with low agro-chemicals dosing also means that the potential loading due to agro-chemicals is quite low. The absence of industries implies that there is no pollution loading from this source as well. Thus it can be concluded that there is no major sources of pollution in Dibang river basin. As a part of the field studies, water samples from the river Dibang at various locations were collected and analysed.

To know the water quality at the Dibang River samples were collected in the study area in the seven different locations, 5 (site 1, 2, 4, 5 & 6) in the upstream and 2 (site 3 & 7) in the downstream for three seasons namely post-monsoon, winter and pre-monsoon seasons in the year 2005-2006 (In September, 2005, October 2005 and February, 2006) . The analysis of the physico-chemical parameters were carried out as per the standard method as cited in Chapter 2 of the report. The results of the analysis are listed in table 3.11. In the tables the values of water analysis is presented as the seasonal mean values.

It is clear from the table 3.9 that that the quality of water of river Dibang is good. The hardness levels indicate the soft quality of water. The low BOD levels indicate the absence of organic pollution source. The other possibility is that since there are no industries in the project area, the major source of organic pollutants is the domestic source. Population density is low in the basin, it can be deduced that the river Dibang has sufficiently large flow so that there is no impact on the river water quality due to disposal of untreated sewage from the settlements. The number of *E. coli* and Coliforms is found to be nil (MPN/100 ml). Thus, the water is not harmful for domestic use. During the socio-economic survey, conducted as a part of the EIA study, the

information on sources of drinking water was also collected. Most of the respondents were using water of adjacent rivers and streams without any disinfection. This is quite likely in a backward, inaccessible area like the proposed project area. However primary treatment such as filtration and boiling of water is recommended before use.

Table 3.11: Water Sampling Report
Sampling Site 1

	pH	EC(mS)	TDS (ppm)	Total Alkalinity	Chloride (ppm) as Cl-	Iron (ppm)	Ca-Hardness (ppm)	Mg-Hardness (ppm)	PO ₄	Mn (ppm)	NO ₃ (ppm)	<i>E. coli</i>	Total Coliform	BOD (mg/l)	COD (mg/l)
Season 1	7.8	0.07	100.00	0.1	0.12	0.01	6.12	0.82	0.99	0	2.6	0	0	0.8	1.8
Season 2	7.5	0.09	200.00	0.9	0.10	0.01	6.04	0.81	0.96	0	2.8	0	0	1.2	2.0
Season 3	7.6	0.08	150.00	0.8	0.11	0.01	6.02	0.78	0.98	0	2.5	0	0	0.5	1.9
BIS Standard	6.5-8.5	7.81	500	200	250	0.3	Total Hardness 300		No std.	0.1	45	0	0	1.8	3.4

Sampling Site 2

	pH	EC (mS)	TDS (ppm)	Total Alkalinity ppm	Chloride (ppm) as Cl-	Iron (ppm)	Ca-Hardness (ppm)	Mg-Hardness (ppm)	PO ₄ (ppm)	Mn (ppm)	NO ₃ (ppm)	<i>E. coli</i>	Total Coliform	BOD (mg/l)	COD (mg/l)
Season 1	7.1	0.04	170	1.1	0.005	0.12	0.42	0.158	1.12	0.002	1.87	0	0	1.3	2.4
Season 2	6.9	0.02	150	1.4	0.004	0.15	0.39	1.154	1.10	0.002	1.92	0	0	1.2	1.0
Season 3	7.2	0.05	160	1.2	0.005	0.12	0.35	1.53	1.10	0.001	1.91	0	0	0.9	1.7
BIS Standard	6.5-8.5	7.81	500	200	250	0.3	Total Hardness 300		No std.	0.1	45	0	0	1.8	3.4

Sampling Site 3

	pH	EC (mS)	TDS (ppt)	Total Alkalinity	Chloride (ppm) as Cl-	Iron (ppm)	Ca-Hardness (ppm)	Mg-Hardness (ppm)	PO ₄	Mn(ppm)	NO ₃ (ppm)	<i>E. coli</i>	Total Coliform	BOD (mg/l)	COD (mg/l)
Season 1	7.5	0.03	150.00	0.4	0.16	0.02	0.86	0.312	0.42	0.001	1.65	0	0	0.8	1.7
Season 2	7.6	0.04	250.00	0.8	0.12	0.04	0.72	0.319	0.45	0.001	1.60	0	0	0.9	1.6
Season 3	7.2	0.02	150.00	0.6	0.12	0.04	0.79	0.325	0.46	0.001	1.48	0	0	0.6	1.5
BIS Standard	6.5-8.5	7.81	500	200	250	0.3	Total Hardness 300		No std.	0.1	45	0	0	1.8	3.4

Sampling Site 4

	pH	EC (mS)	TDS (ppm)	Total Alkalinity	Chloride (ppm) as Cl-	Iron (ppm)	Ca-Hardness (ppm)	Mg-Hardness (ppm)	PO ₄	Mn (ppm)	NO ₃ (ppm)	<i>E. coli</i>	Total Coliform	BOD (mg/L)	COD (mg/L)
Season 1	7.2	0.05	100.00	0.3	0.15	0.02	0.9	0.32	0.63	0.002	1.4	0	0	0.8	1.8
Season 2	7.4	0.04	200.00	0.6	0.16	0.03	2.04	0.51	0.72	0.001	1.5	0	0	1.2	2.0
Season 3	7.3	0.56	150.00	0.7	0.10	0.05	3.02	0.42	0.56	0.002	2.3	0	0	0.5	1.9
BIS Standard	6.5-8.5	7.81	500	200	250	0.3	Total Hardness 300		No std.	0.1	45	0	0	1.8	3.4

Sampling Site 5

	pH	EC (mS)	TDS (ppm)	Total Alkalinity	Chloride (ppm) as Cl-	Iron (ppm)	Ca-Hardness (ppm)	Mg-Hardness (ppm)	PO ₄	Mn (ppm)	NO ₃ (ppm)	<i>E. coli</i>	Total Coliform	BOD (mg/l)	COD (mg/l)
Season 1	7.8	0.07	100.00	0.1	0.12	0.01	6.12	0.82	0.99	0.002	2.1	0	0	0.8	1.8
Season 2	7.5	0.09	200.00	0.9	0.10	0.01	6.04	0.81	0.96	0	2.9	0	0	1.2	2.0
Season 3	7.6	0.08	150.00	0.8	0.11	0.01	6.02	0.78	0.98	0	3.2	0	0	0.5	1.9
BIS Standard	6.5-8.5	7.81	500	200	250	0.3	Total Hardness 300		No std.	0.1	45	0	0	1.8	3.4

Sampling Site 6

	pH	EC(m S)	TDS (ppm)	Total Alkalinity	Chloride (ppm) as Cl-	Iron (ppm)	Ca-Hardness (ppm)	Mg-Hardness (ppm)	PO ₄	Mn (ppm)	NO ₃ (ppm)	<i>E. coli</i>	Total Coliform	BOD (mg/l)	COD (mg/l)
Season 1	7.1	0.04	140.00	0.4	0.12	0.02	5.09	0.52	0.39	0.003	2.2	0	0	0.8	1.8
Season 2	7.5	0.05	210.00	0.5	0.18	0.06	6.11	0.60	0.52	0.002	2.1	0	0	1.2	2.0
Season 3	7.2	0.06	180.00	0.2	0.11	0.01	6.01	0.46	0.38	0.003	2.8	0	0	0.5	1.9
BIS Standard	6.5-8.5	7.81	500	200	250	0.3	Total Hardness 300		No std.	0.1	45	0	0	1.8	3.4

Sampling Site 7

	pH	EC (mS)	TDS (ppm)	Total Alkalinity	Chloride (ppm) as Cl-	Iron (ppm)	Ca-Hardness (ppm)	Mg-Hardness (ppm)	PO ₄	Mn (ppm)	NO ₃ (ppm)	<i>E. coli</i>	Total Coliform	BOD (mg/l)	COD (Mg/l)
Season 1	7.3	0.06	110.00	0.1	0.12	0.01	6.12	0.82	0.99	0	2.6	0	0	0.8	1.8
Season 2	7.9	0.05	210.00	0.9	0.10	0.01	6.04	0.81	0.96	0	2.8	0	0	1.2	2.0
Season 3	7.2	0.08	170.00	0.8	0.11	0.01	6.02	0.78	0.98	0	2.5	0	0	0.5	1.9
BIS Standard	6.5-8.5	7.81	500	200	250	0.3	Total Hardness 300		No std.	0.1	45	0	0	1.8	3.4

Site1 – Near Ithun Bridge; Site 2 – Near Tangon River Bridge ; Site 3 – Downstream of Dam Site; Site 4- Kronli; Site 5 – Munli camp; Site 6- Emra R.; Site 7 - Dambuk



3.8 SOIL CHARACTERISTICS

The soil type of the directly draining catchment has been classified as per the National Bureau of Soil Survey & Landuse Planning (NBSS & LUP). Soil details of directly draining area are shown in Table 3.12. Soil map of directly draining catchment is placed as Map 3.4.

Table 3.12: Soil Details of Directly Draining Catchment

Sl. No.	Mapping Unit (As per NBSS & LUP)	Soil Description	Association with	Erositivity	Area (ha)
1	1	Shallow, excessively drained, loamy-skeletal	Moderately deep, excessively drained on moderately steep slope	Very severe	11151.52
2	2	Deep, loamy-skeletal	Deep, somewhat excessively drained loamy skeletal on moderately steep slope	Severe	1211.68
3	3	Shallow, loamy-skeletal	Moderately deep, somewhat excessively drained on moderately steep slope	Severe	11254.12
4	4	Shallow, loamy-skeletal	Moderately deep, somewhat excessively drained on very steep slope	Severe	21553.76
5	7	Very deep, fine soils	Moderately shallow, excessively drained clayey soils on steep slope	Severe	184.64

6	9	Deep, well drained fine soils	Very deep, well-drained, fine loamy soils on moderate slope	Moderate	7371.44
7	11	Very deep, well drained, fine loamy soils	On moderate slope, very deep well drained fine soils	Moderate	3389.12
8	46	Rocky mountains covered with perpetual snow and glaciers	-	-	3695.6
Total					59811.88

3.8.1 Soil Quality

The samples were collected from three different locations as per the methodology described in Chapter 2 of the report. Site wise soil quality analysis details are given in the following tables:

Table 3.13: Soil Sample Analysis Report

Sampling Site 1

	Location of the samples	Positions	Altitude	pH	Organic Carbon (%)	Texture (Sand / silt / clay)	Dispersion Ratio
Season 1	Near Apruli Cane Bridge	28°35.47' N 95°50.45' E	2264 ft.	4.6	1.8	74.72 / 24.74 / 1.14	39.8 : 36.26
Season 2	Near Apruli Cane Bridge	28°35.47' N 95°50.45' E	2264 ft.	4.5	1.9	79.18 / 25.00 / 1.82	42.6 : 38.16
Season 3	Near Apruli Cane Bridge	28°35.47' N 95°50.45' E	2264 ft.	4.6	1.5	75.72 / 24.10 / 0.18	40.16 : 32.24
Mean Values				4.6	1.7		

	Nitrogen (ppm)	Phosphorous (ppm)	Potassium (ppm)	Iron (ppm)	Copper (ppm)	Manganese (ppm)	Zinc (ppm)	Electrical Conductivity (mmho/cm)	Porosity (%)
Season 1	120.8	9.9	61.1	2.3	0.6	1.1	0.0446	0.4	55.67
Season 2	170.7	7.7	42.9	1.9	ND	0.9	0.0223	0.5	40.57
Season 3	127.7	9.0	53.8	2.0	ND	0.8	0.0357	0.2	53.69
Mean Values	130.4	8.9	52.5	2.1	0.2	0.9	0.0357	0.4	49.98

Sampling Site 2

	Location of the samples	Positions	Altitude	pH	Organic Carbon (%)	Texture (sand / silt / clay)	Dispersion Ratio
Season 1	Near Damsite	28°20.55' N 95°46.45' E	1295 ft.	5.2	1.5	58.26 / 27.24 / 14.5	25.42 : 32.14
Season 2	Near Damsite	28°20.51'N 95°46.43'E	1274 ft	5.1	1.8	65.12 / 22.4 / 12.48	32.10 : 29.42
Season 3	Near Damsite	28°20.52'N 95°46.41' E	1226 ft	4.8	1.6	68.14 / 14.6 / 17.26	30.12 : 30.6
Mean Values				5.0	1.6		

	Nitrogen (ppm)	Phosphorous (ppm)	Potassium (ppm)	Iron (ppm)	Copper (ppm)	Manganese (ppm)	Zinc (ppm)	Electrical Conductivity (mmho/cm)	Porosity (%)
Season 1	112.9	9.0	68.5	1.7	ND	1.0	0.067	0.3	54.06
Season 2	94.4	10.3	50.3	1.5	ND	0.9	0.058	0.2	54.26
Season 3	159.0	8.2	58.2	1.8	ND	0.9	0.049	0.3	51.80
Mean Values	122.1	9.2	59.0	1.7	ND	0.9	0.058	0.3	53.40

Sampling Site 3

	Location of the samples	Positions	Altitude	pH	Organic Carbon (%)	Texture (sand/silt/clay)	Dispersion Ratio
Season 1	Near Ithun River Bridge	28°22.40' N 95°55.80' E	2217 ft.	5.0	1.2	56.26/22.24/12.5	25.42 : 32.14
Season 2	Near Ithun River Bridge	28°22.40' N 95°55.80' E	2217 ft.	4.6	1.6	60.12/21.4/10.48	32.10 : 29.42
Season 3	Near Ithun River Bridge	28°22.40' N 95°55.80' E	2217 ft.	4.2	1.4	61.11/18.2/12.21	30.12 : 30.6
Mean Values				5.0	1.4		

	Nitrogen (ppm)	Phosphorous (ppm)	Potassium (ppm)	Iron (ppm)	Copper (ppm)	Manganese (ppm)	Zinc (ppm)	Electrical Conductivity (mmho/cm)	Porosity (%)
Season 1	110.9	9.0	68.5	1.7	ND	1.0	0.067	0.3	54.06
Season 2	94.4	10.3	50.3	1.5	ND	0.9	0.058	0.2	54.26
Season 3	159.0	8.2	58.2	1.8	ND	0.9	0.049	0.3	51.80
Mean Values	122.1	9.2	59.0	1.7	ND	0.9	0.058	0.3	53.40

The soils of the catchment are acidic in nature (pH values ranges from 4.1 to 4.8), which is favorable for growth of citrus species. The organic carbon content is also reasonably higher this is probably due to the presence of decomposed leaf litter. The organic carbon content indicates the suitability of growing of plant species. The texture of soil is sandy loam and the porosity is medium, which indicates the soil is moderately permeable and the water holding capacity of soil is also not less. The subsurface drainage is not severe. The land capability classification is based on the soil physico-chemical parameters.

3.8.2 Inference

Sampling Site 1

Soil pH ranges from 4.5 – 4.6 & is very strongly acidic with presence of free acids & likely occurrence of exchangeable Aluminum. Molybdenum, Ca & Mg deficiency is a major problem of this type of soils. Liming may be done. Organic carbon content is high (1.5-1.8%) & is good. Regarding Texture soil is sandy loam. If dispersion ratio is >8, it is assumed that Hydraulic conductivity rate is very low. Electrical Conductivity is normal & porosity is good for drainage.

Nitrogen level is normal & good. Phosphorous level is deficient & Potassium level is low to deficient. Micronutrients Mn, Zn, Cu are found to be low to deficient except Iron.

Sampling Site 2

Soil is sandy loam with presence of free acids & likely occurrence of exchangeable Aluminum. From dispersion ratio it is assumed that Hydraulic conductivity is very low. Electrical Conductivity is normal & porosity is good for drainage. This soil is good for agriculture and horticulture crops & pH shows strongly acidic nature and also the organic carbon content is very good. Nitrogen level is normal & good. Phosphate level is deficient & Potassium level is low to deficient. Micronutrients Mn, Zn, Cu are found to be low to deficient except Iron.

Crops that can be grown are Rice, Wheat, Maize, Mustard, Sugar cane (in

site II) etc. fruit crops like Citrus, Lemon, Banana, Pineapple, Litchi etc.

Sampling Site 3

Soil pH ranges from 4.2 – 5.0 & is very acidic with presence of free acids & likely occurrence of exchangeable Aluminum. Molybdenum, Ca & Mg deficiency is a major problem of this type of soils. Liming may be done. Organic carbon content is good (1.2-1.6%) & is good. Regarding Texture, soil is sandy loam. If dispersion ratio is >8, it is assumed that Hydraulic conductivity rate is very low. Electrical Conductivity is normal & porosity is good for drainage.

Nitrogen level is normal & good. Phosphate level is deficient & Potassium level is low to deficient. Micronutrients Mn, Zn, Cu are found to be low to deficient except Iron.

3.9 AMBIENT AIR & NOISE QUALITY

3.9.1 Ambient Air Quality

The results of ambient air quality monitoring survey are summarized in table 3.14. The project area can be categorized as residential and rural areas. It is clear from table 3.14 that the concentrations of SPM, SO_x, NO_x and CO are much below the standard values. Hence, the ambient air quality in the project area is good.

3.9.2 Noise Quality

The result of noise quality analysis is given in table 3.15. It is clear from the table 3.15, it is found that the noise level in the project area is far below the prescribed limit. This is because the population density in the area is very low and there is hardly any developmental activity in the project area at present.

Table 3.14: Ambient Air Quality Test Report

Sampling Site 1 (24 hourly sampling data)

	Location of the samples	Positions	Altitude	SPM ($\mu\text{g}/\text{m}^3$)	SOx ($\mu\text{g}/\text{m}^3$)	NOx ($\mu\text{g}/\text{m}^3$)	CO ($\mu\text{g}/\text{m}^3$)
Season 1	Near Damsite	28°20.55' N 95°46.45' E	1295 ft.	70	8.3	9.6	BDL
Season 2	Near Damsite	28°20.51'N 95°46.43'E	1274 ft	80	10.4	11.7	BDL
Season 3	Near Damsite	28°20.52'N 95°46.41' E	1226 ft	56	7.0	7.7	BDL
Mean Values				69	8.6	9.7	-
BIS standard				200	80	80	4.00

Sampling site 2 (24 hourly sampling data)

	Location of the samples	Positions	Altitude	SPM $\mu\text{g}/\text{m}^3$	SOx $\mu\text{g}/\text{m}^3$	NOx $\mu\text{g}/\text{m}^3$	CO $\mu\text{g}/\text{m}^3$
Season 1	Near Apruli Cane Bridge	28°35.47' N 95°50.45' E	2264 ft.	97	11.6	9.8	1.0
Season 2	Near Apruli Cane Bridge	28°35.47' N 95°50.45' E	2264 ft.	89	9.4	11.7	1.2
Season 3	Near Apruli Cane Bridge	28°35.47' N 95°50.45' E	2264 ft.	106	9.0	6.0	0.7
Mean Values				97	10	9.1	0.96
BIS standard				200	80	80	4.00

Sampling Site 3 (24 hourly sampling data)

	Location of the samples	Positions	Altitude	SPM µg/m ³	SOx µg/m ³	NOx µg/m ³	CO µg/m ³
Season 1	Near Ithun River Bridge	28°22.41' N 95°55.82' E	2248 ft.	58	5.0	6.0	BDL
Season 2	Near Ithun River Bridge	28°22.40' N 95°55.80' E	2217 ft.	62	10.5	6.2	BDL
Season 3	Near Ithun River Bridge	28°22.42' N 95°55.75' E	2204 ft.	56	8.0	7.0	BDL
Mean Values				59	7.8	6.4	BDL
BIS standard				200	80	80	4.00

Table 3.15: Noise Quality Analysis Report

	Location of the samples	Positions	Altitude	Site 1 In dB		Site 2 In dB		Site 3 In dB	
				Leq*	Range	Leq*	Range	Leq*	Range
Season 1	Near Apruli Cane Bridge	28°35.48' N 95°50.47' E	2284 ft.	45	38-49	47	42-52	36	32-45
Season 2	Near Apruli Cane Bridge	28°35.47' N 95°50.45' E	2264 ft.	43	36-49	47	43-30	38	32-47
Season 3	Near Apruli Cane Bridge	28°35.49' N 95°50.43' E	2247 ft.	40	34-46	42	40-50	38	34-45
Mean Values				43		45		37	

* Log Equivalent